Supporting Information for paper entitled: *"Single-molecule FRET studies of the cooperative and non-cooperative binding kinetics of the bacteriophage T4 single-stranded DNA binding protein (gp32) to ssDNA lattices at replication fork junctions"*, by Wonbae Lee, John P. Gillies, Davis Jose, Brett A. Israels, Peter H. von Hippel and Andrew H. Marcus.

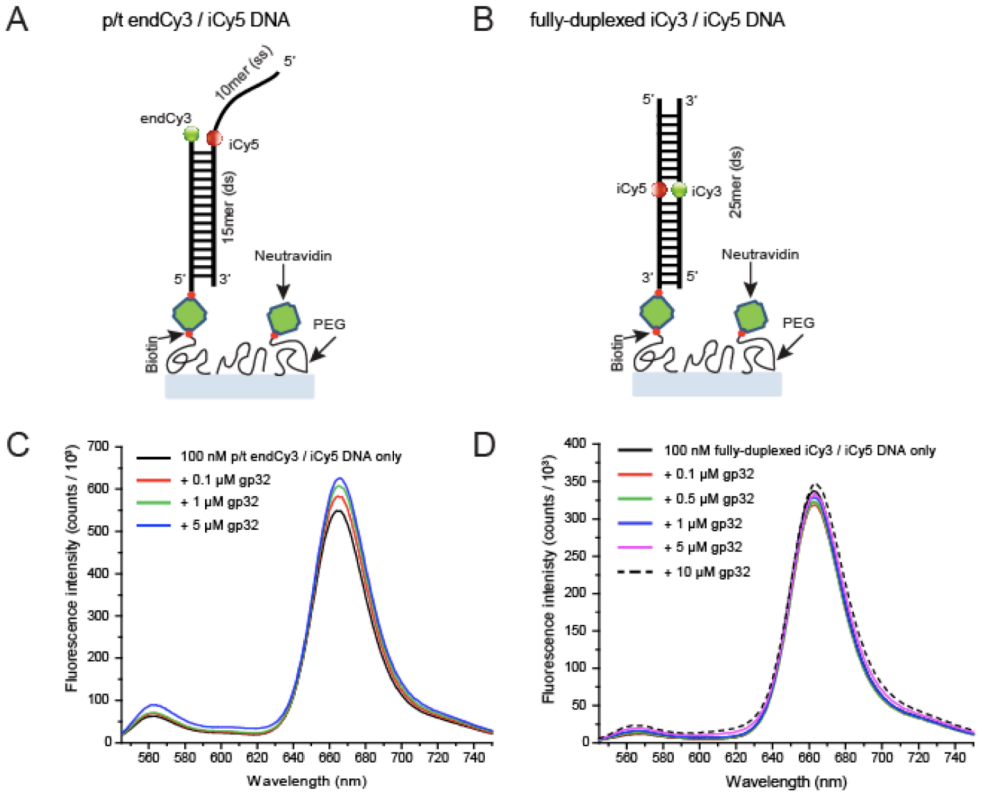

Figure S1. ***DNA constructs used for control bulk FRET experiments***. (*A*) In this primer / template (p/t) DNA construct, the Cy3 chromophore is attached to the 3'-terminus of the primer strand and the Cy5 chromophore is internally positioned within the template strand near the p/t junction. (*B*) The Cy3 and Cy5 chromophores are incorporated into the sugar-phosphate DNA backbone using phosphoramidite chemistry at the middle of duplex. Bulk FRET measurements were performed to see whether the FRET signal changed upon addition of gp32 (*C*) with the primer / template (p/t) DNA construct shown in Fig. S1A, and (*D*) with the fully duplexed DNA construct shown in Fig. S1B. The protein concentration dependent changes in FRET signal observed for these control substrates are small in comparison to those we observed for most of the substrates investigated in this work.

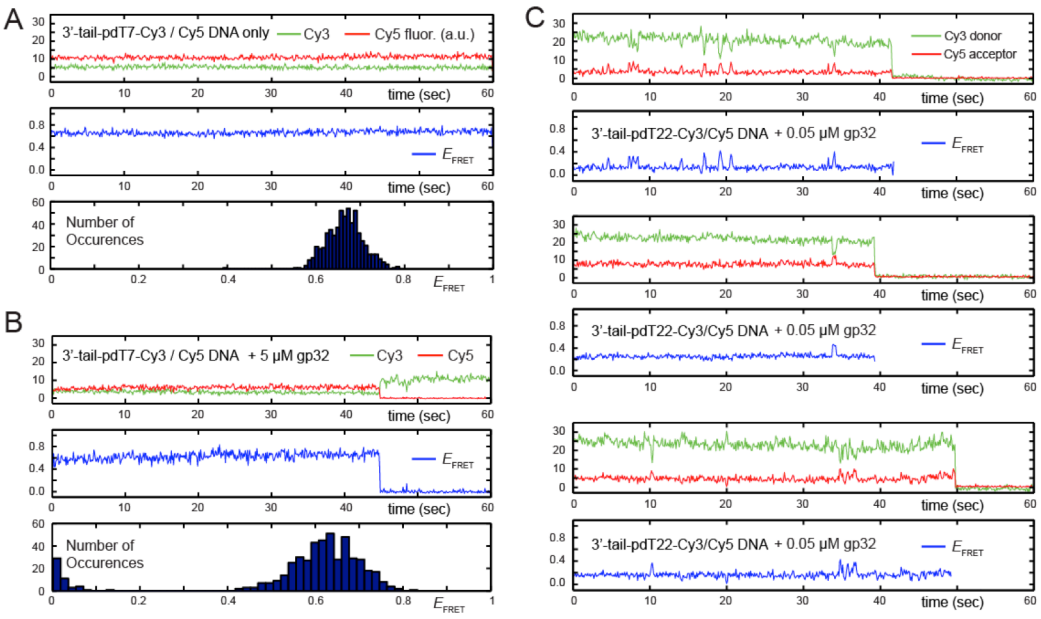

Figure S2. Representative smFRET data for p(dT)$_7$– and p(dT)$_{22}$–tail p/t DNA constructs. (*A*) Representative smFRET trace of the 3'-tail-pdT7-Cy3/Cy5 construct. (*B*) Representative smFRET trace of the 3'-tail-pdT7-Cy3/Cy5 construct incubated with 5 µM gp32. (*C*) Representative traces of the 3'-tail-pdT22-Cy3/Cy5 construct incubated in a flow chamber with 0.05 µM gp32, and showing the effects of cooperative binding of three gp32 proteins. All samples were incubated in 100 mM NaCl, 6 mM $MgCl_2$ and 10 mM Tris at pH 8.0.

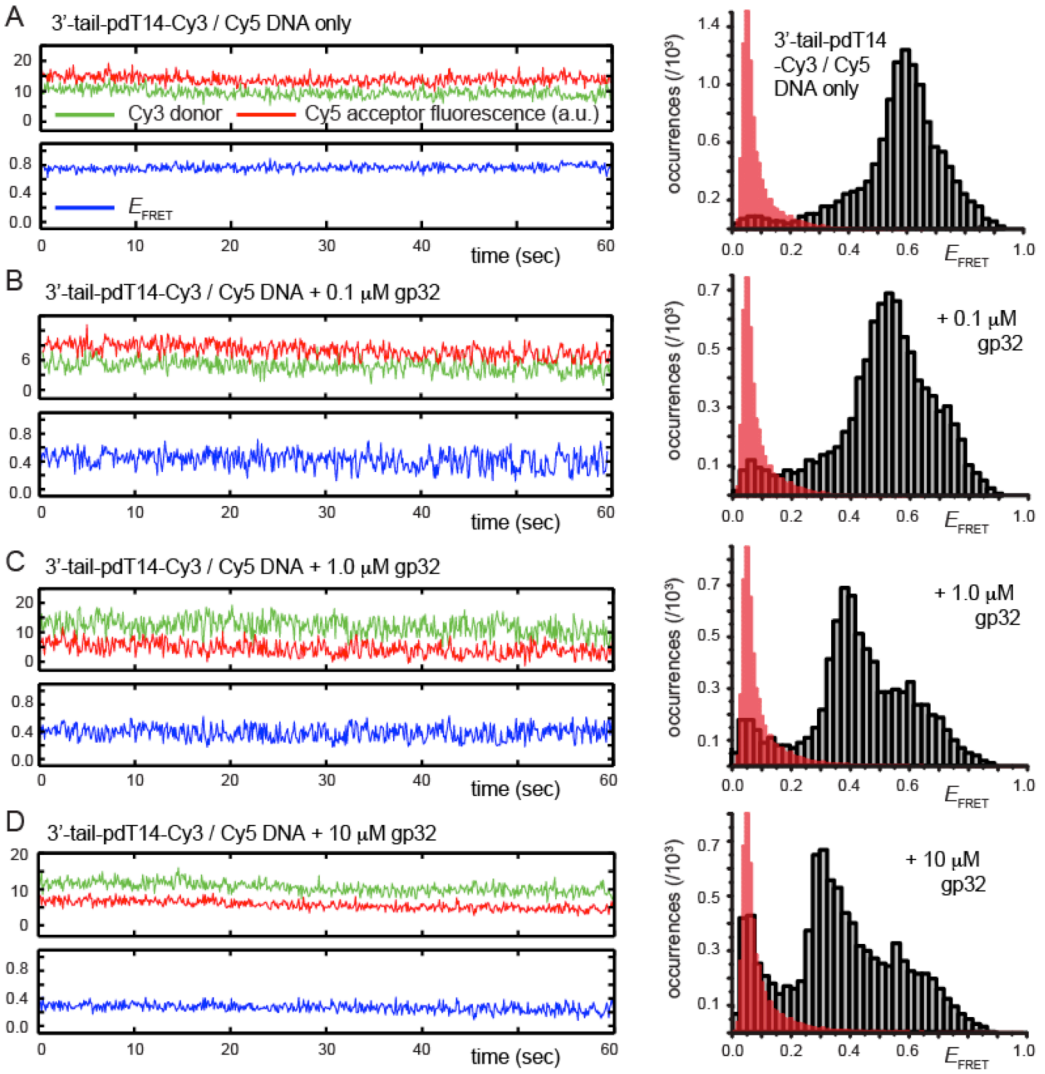

Figure S3. Representative smFRET trajectories of the 3'-tail-pdT14-Cy3/Cy5 p/t DNA substrate at various gp32 concentrations. (*A*) p/t DNA substrates alone; (*B*) in the presence of 0.1 μM gp32; (*C*) 1.0 μM gp32; and (*D*) 10 μM gp32. Histograms of the smFRET efficiencies [$E_{FRET} = I_A/(I_D + I_A)$], which are based on the compilation of thousands of individual smFRET trajectories, are shown in the right column. Cy3 and Cy5 fluorescence levels have been vertically displaced to clearly display anti-correlated signal fluctuations. The red-shaded regions in the histograms show the probability distribution of background signals, which was determined from control measurements performed using biotin-Cy3 samples (see Fig. S7). The buffer solution in this and the subsequent figures, unless otherwise noted, contained 100 mM NaCl, 6 mM $MgCl_2$ and 10 mM Tris at pH 8.0.

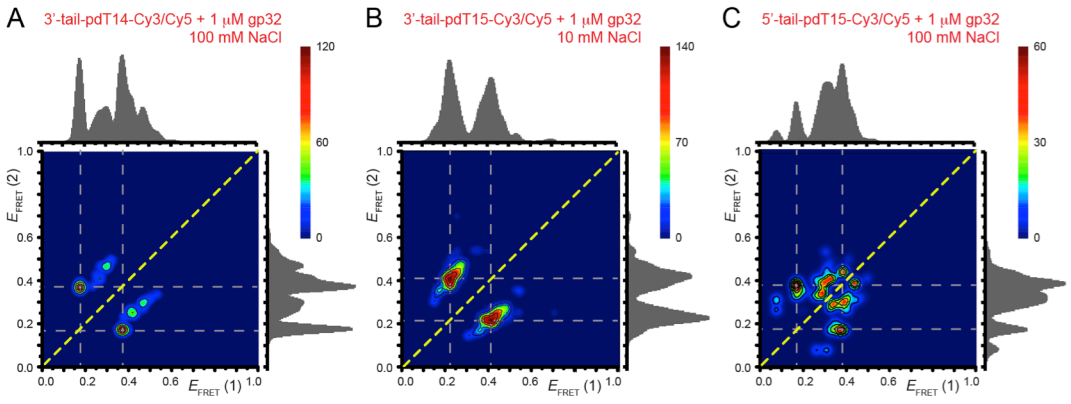

Figure S4. Cumulative TDPs constructed from the sum of ~50 molecular trajectories from (*A*) the 3'-tail-pdT14-Cy3/Cy5 DNA in the presence of 1 μM gp32 and 100 mM NaCl; (*B*) the 3'-tail-pdT15-Cy3/Cy5 DNA in the presence of 1 μM gp32 and 10 mM NaCl; and (*C*) the 5'-tail-pdT15-Cy3/Cy5 DNA in the presence of 1 μM gp32 and 100 mM NaCl. Integrated transition density distributions are shown (in gray) projected along the horizontal and vertical axes. Horizontal and vertical gray dashed line segments connecting low- and high-E_{FRET} values indicate the most prominent state-to-state transition pathways. The multiple features that appear very close to the diagonal in *Panel C* lie outside of the range of experimental accuracy, and are thus not interpreted (see Fig. S7).

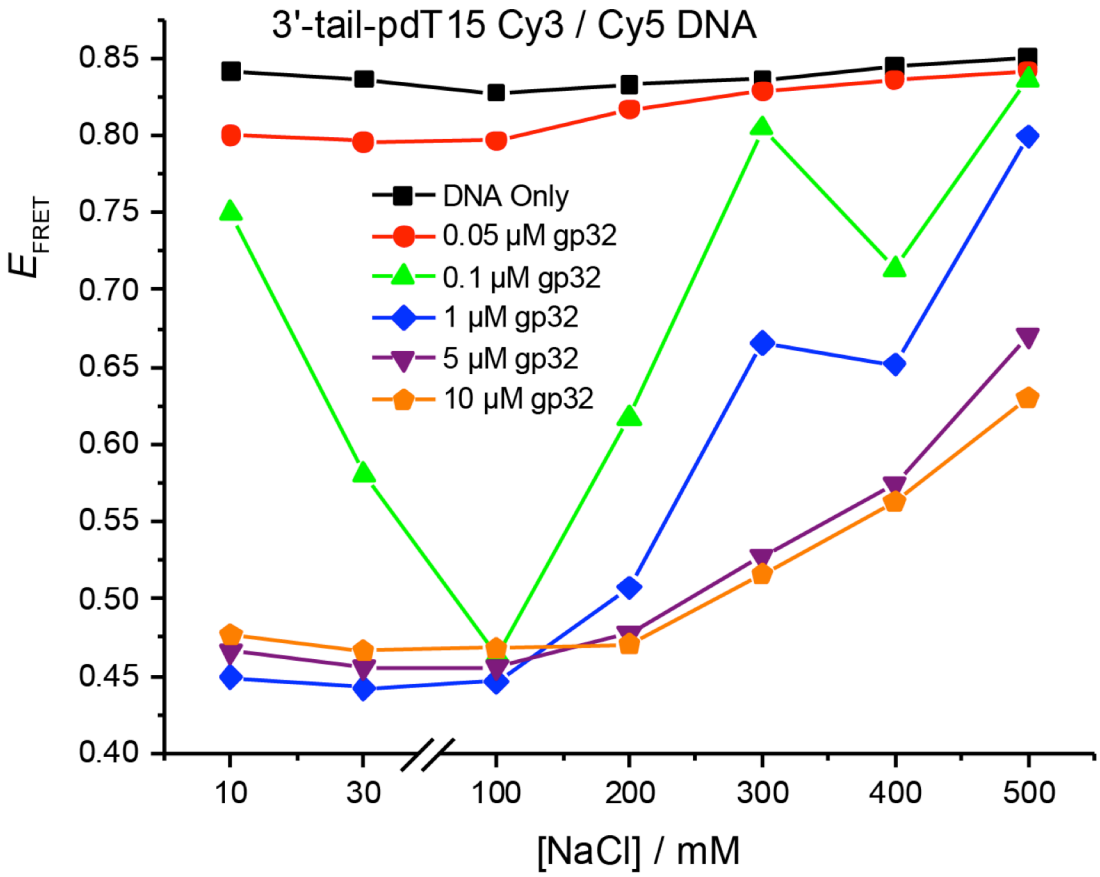

Figure S5. Bulk FRET measurements for the 3'-tail-pdT15-Cy3/Cy5 construct (starting at 100 nM) at various NaCl concentrations, 6 mM $MgCl_2$, and mM Tris at pH 8.0, and as a function of gp32 concentration. Note that the horizontal scale is expanded for the first two data points for purposes of visualization.

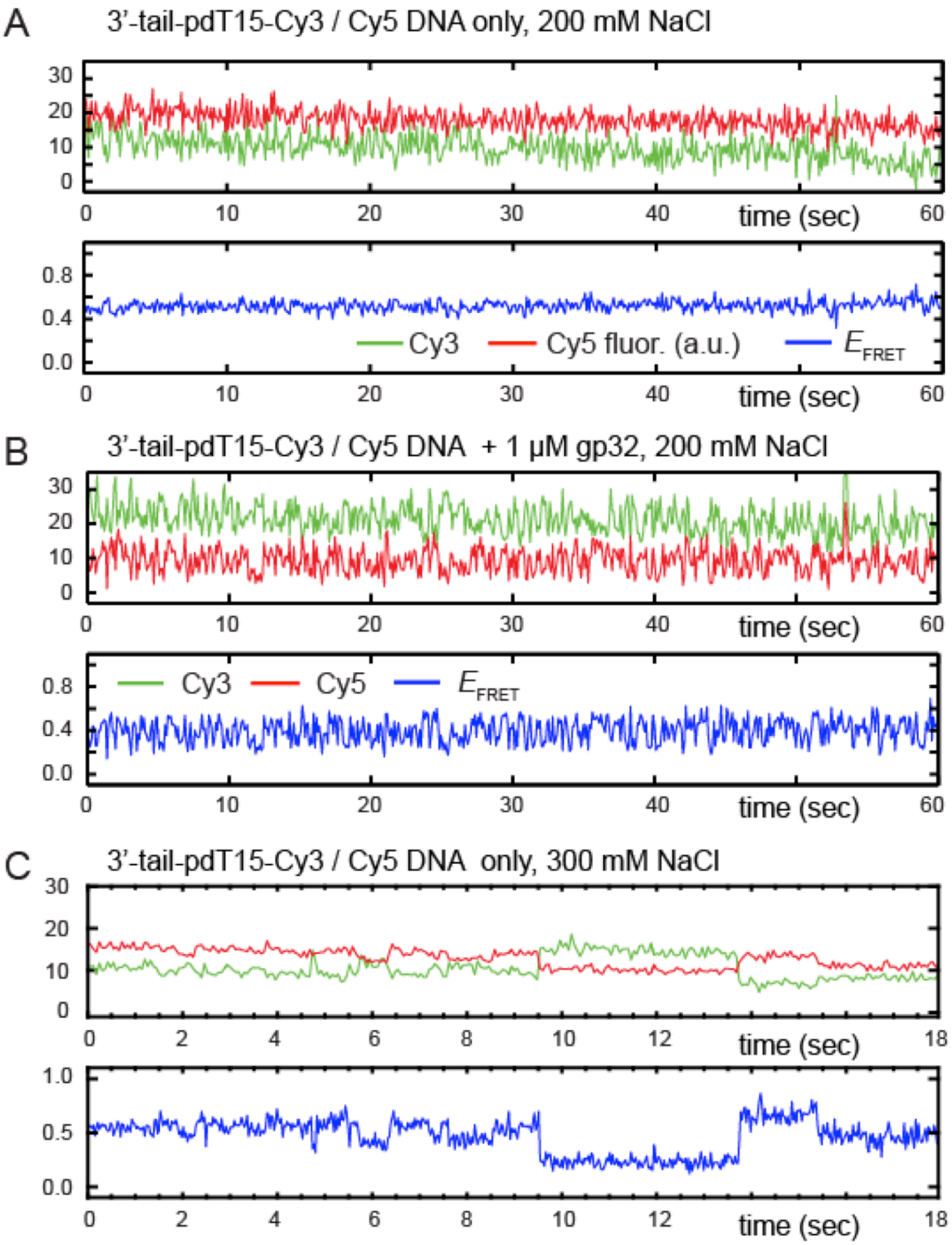

Figure S6. Representative **smFRET traces of the 3'-tail-pdT15-Cy3/Cy5 construct at elevated NaCl concentrations, 6 mM $MgCl_2$, and mM Tris at pH 8.0** (*A*) p/t DNA only at 200 mM NaCl, (*B*) in the presence of 1 μM gp32 at 200 mM NaCl, and (*C*) p/t DNA only at 300 mM NaCl. Cy3 and Cy5 fluorescence levels have been vertically displaced to clearly display the anti-correlated signal fluctuations.

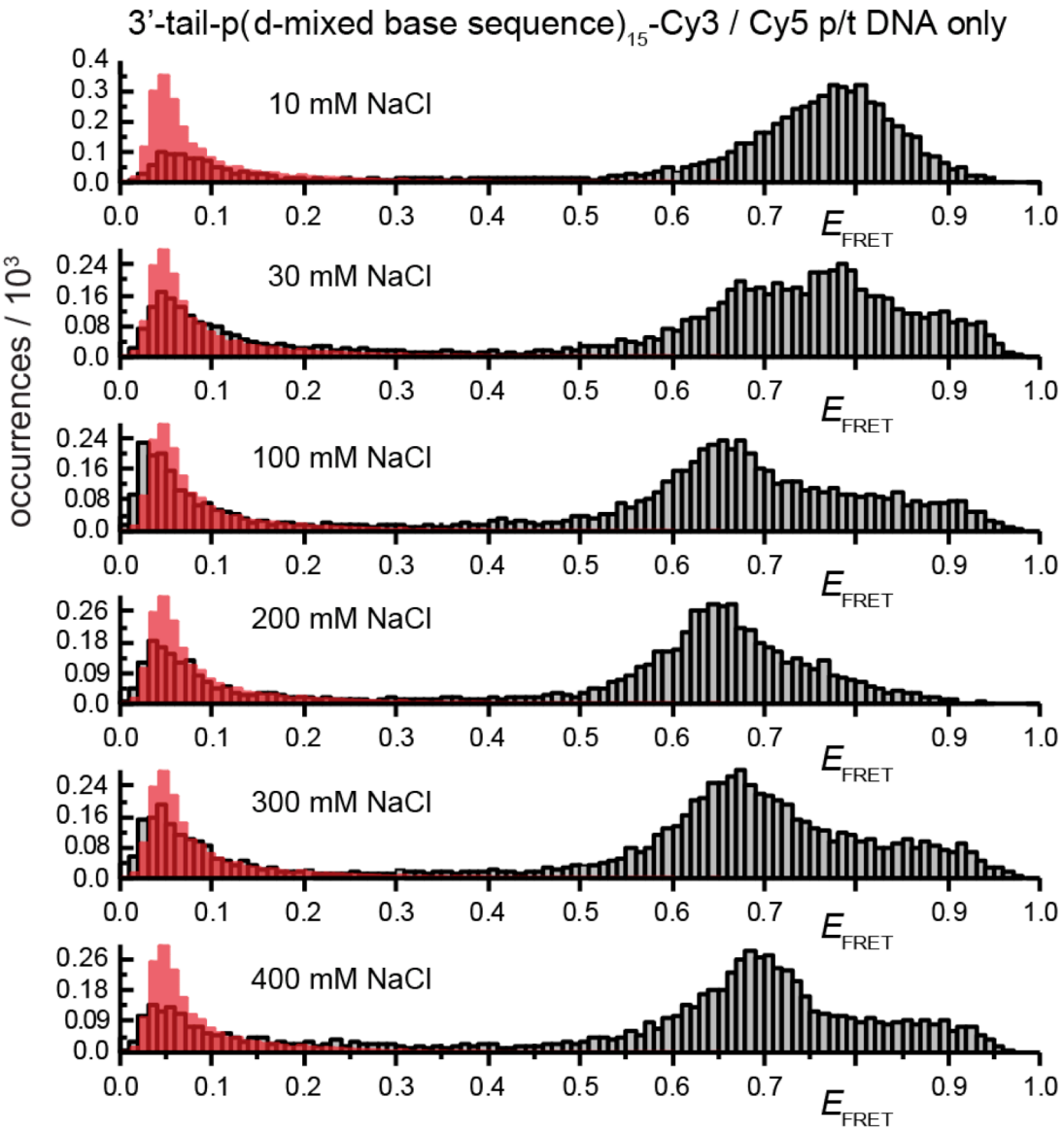

Figure S7. FRET efficiency histograms of the 3'-tail-pd(mixed-base-sequence)15-Cy3/Cy5 construct at various NaCl concentrations, 6 mM $MgCl_2$ and mM Tris at pH 8.0. The red-shaded regions in the histograms show the probability distribution of background signals, which was determined from control measurements performed using biotin-Cy3 samples (see Fig. S8). While the mixed-base-sequence does not exhibit the feature seen at $E_{FRET} \sim 0.36$ for the 3'-tail-pdT15-Cy3/Cy5 constructs at elevated salt, the high-FRET feature ($0.5 < E_{FRET} < 0.95$) for this construct appears to change shape as a function of salt concentration.

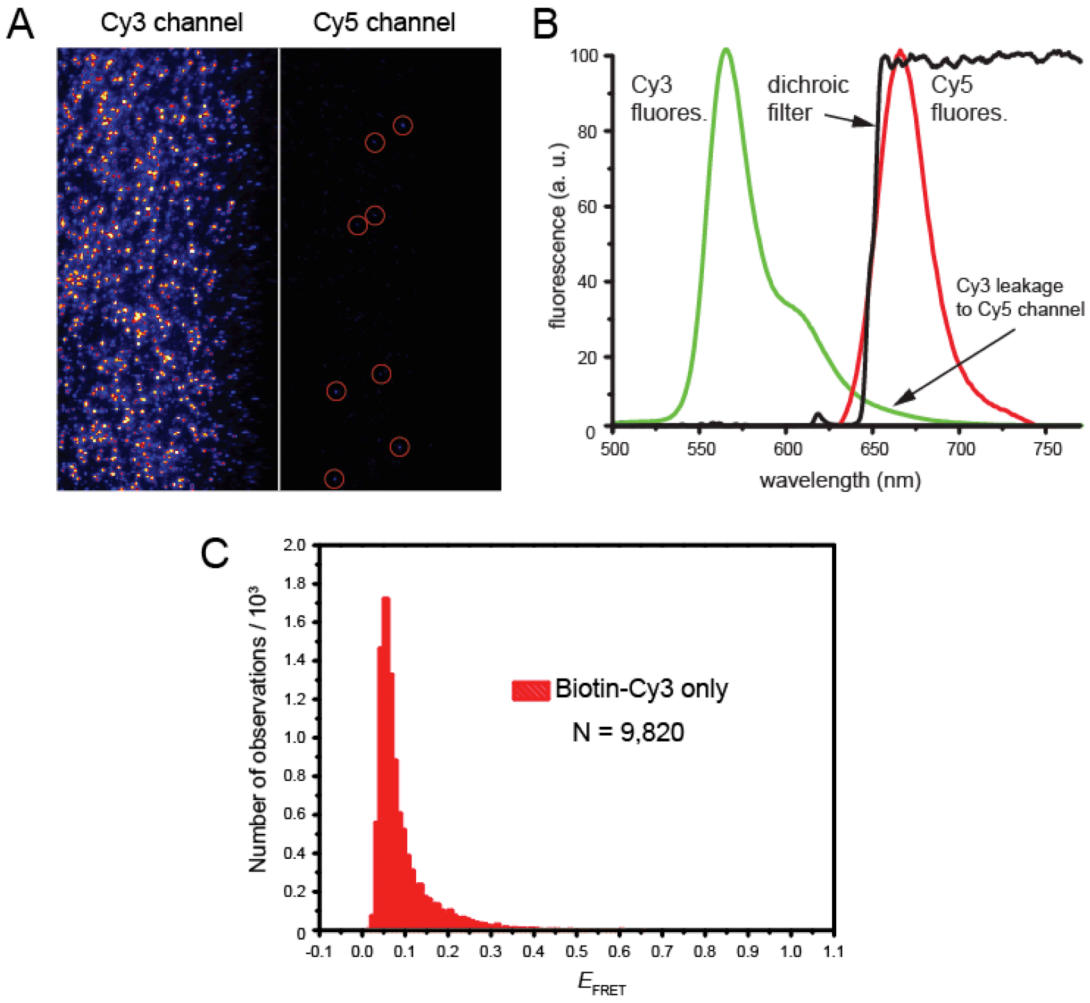

Figure S8. Calibration measurements for single-molecule FRET efficiency histograms. All E_{FRET} histograms shown in this work exhibit an artifact feature peaked at ~ 0.07. The artifact is due to the presence of Cy3/Cy5 DNA constructs in which the Cy5 has become optically inactive. The effect of inactive Cy5 on our histograms was determined by performing control measurements on samples labeled with Cy3 only. (*A*) Split screen fluorescence image of a sample labeled with Biotin-Cy3, which was obtained with the smFRET instrument used in the current studies. The left side of the image shows the image of the Cy3 fluorescence. The right side shows the 'ghost' images of partial Cy3 fluorescence that penetrates the dichroic filter, and is detected in the Cy5 channel. The most prominent 'ghost' features are highlighted with red circles. (*B*) Fluorescence spectra of the Cy3 and Cy5 chromophores superimposed with the dichroic filter used in our experiments (catalog no. FF650-Di01-25x36, Semrock). A small amount of Cy3 fluorescence (~ 10%) leaks through the dichroic mirror, and is detected within the Cy5 channel. (*C*) When the image processing software and protocol is applied to these test measurements, the resulting E_{FRET} histogram exhibits a single broad feature peaked at ~ 0.07. Further details about the instrumentation used in these studies are described in Ref. (6) of the text.

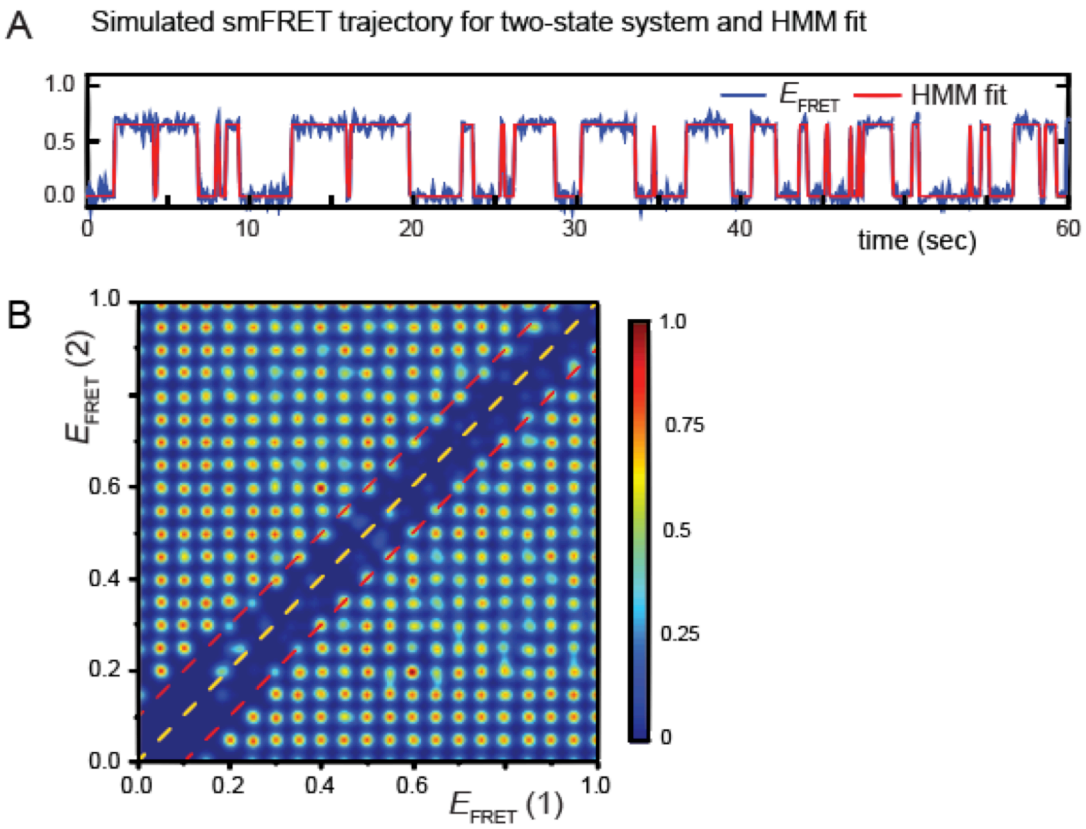

Figure S9. Test calculations showing the accuracy of the Hidden Markov Modeling (HMM) procedure, and its use in constructing Transition Density Plots (TDPs). Simulated smFRET trajectories with pre-selected values for initial and final FRET values were used as input to the HMM analysis software. 420 trajectories were generated with initial and final FRET values varied by 0.05 increments, over the range 0.0 – 1.0. All trajectories assumed a 4% level of noise. (*A*) An example of one such simulated smFRET trajectory, and the resulting HMM fit, is shown for the case with $E_{FRET}(1)$ = 0.0 and $E_{FRET}(2)$ = 0.65. (*B*) The results of the HMM analysis applied to the array of 20 × 20 = 400 simulated trajectories. These model calculations show that the HMM analysis employed throughout this work can reliably identify transitions between initial and final FRET values with magnitudes $\Delta E_{FRET} = |E_{FRET}(2) - E_{FRET}(1)| \geq 0.1$ for $E_{FRET}(1)$, $E_{FRET}(2) \geq 0.3$. Simulated transitions with magnitudes less than 0.1 were not reliably recognized, and gave rise to the darkened region of the TDP between the red-dashed diagonal lines. We further note that this accuracy was reduced for trajectories with initial and final values $E_{FRET}(1), E_{FRET}(2) \leq 0.3$, in which case the HMM analysis could only identify transitions with magnitudes $\Delta E_{FRET} \geq 0.15$

Table S1. 0.1 μM gp32 HMM persistence times $\langle\tau\rangle_{m-\mathrm{bound}}$ and apparent equilibrium constants, $K_{app} = [2-\mathrm{bound}] \,/\, [0-\mathrm{bound}]$.

Substrate & [NaCl]	m, No. of gp32 molecules bound	$\langle\tau\rangle_{m-\mathrm{bound}}$ (s)	K_{app}	Number of Molecules
3' 15-mer	2	0.32	0.24	50
100 mM NaCl	0	1.31		
3' 15-mer	2	0.76	3.8	50
10 mM NaCl	0	0.20		
5' 15-mer	2	0.26	0.26	40
100 mM NaCl	0	0.97		
3' 14-mer	2	0.24	0.16	50
100 mM NaCl	0	1.44		

Table S2. 1 μM gp32 HMM persistence times $\langle\tau\rangle_{m-\mathrm{bound}}$ and apparent equilibrium constants, $K_{app} = [2-\mathrm{bound}] \,/\, [0-\mathrm{bound}]$.

Substrate & [NaCl]	m, No. of gp32 molecules bound	$\langle\tau\rangle_{m-\mathrm{bound}}$ (s)	K_{app}	Number of Molecules
3' 15mer	2	0.51	3.2	33
100 mM NaCl	0	0.16		
3' 15mer	2	0.96	9.6	47
10 mM NaCl	0	0.10		
5' 15mer	2	0.26	0.48	36
100 mM NaCl	0	0.54		
3' 14mer	2	0.31	0.22	32
100 mM NaCl	0	1.40		